IEEE Access
Multidisciplinary ⋮ Rapid Review ⋮ Open Access Journal

Received November 27, 2018, accepted December 5, 2018, date of publication December 17, 2018, date of current version January 11, 2019.

Digital Object Identifier 10.1109/ACCESS.2018.2886289

Health Status Prediction Based on Belief Rule Base for High-Speed Train Running Gear System

CHAO CHENG[1,2,3], JIUHE WANG[1], WANXIU TENG[2], MINGLIANG GAO[2,3], BANGCHENG ZHANG[4], XIAOJING YIN[4], AND HAO LUO[5]

[1]School of Computer Science and Engineering, Changchun University of Technology, Changchun 130012, China
[2]National Engineering Laboratory, CRRC Changchun Railway Vehicles Co., Ltd., Changchun 130062, China
[3]Department of Automation, Tsinghua University, Beijing 100084, China
[4]School of Mechatronic Engineering, Changchun University of Technology, Changchun 130012, China
[5]Academy of Astronautics, Harbin Institute of Technology, Harbin 150001, China

Corresponding author: Bangcheng Zhang (zhangbangcheng@ccut.edu.cn)

This work was supported in part by the National Natural Science Foundation of China under Grant 61751304 and Grant 61803044, in part by the Key Science and Technology R&D Project of the Jilin Science and Technology Department under Grant 20180201125GX and Grant 20160520020JH, and in part by the Project of Educational Commission of Jilin Province of China under Grant JJKH20191287KJ and Grant 2016342.

ABSTRACT The running gear is a vital component of a high-speed train to ensure operation safety. Accurately predicting the future health status of the running gear is significant to keep the reliability and safety of trains. It is difficult to predict the future health status based on the analytical model of the running gear system because of its complexity and coupling. Moreover, the fault data are a minor part of tremendous data in the running and monitoring process of a high-speed train, which obstructs accurately predicting the health status based on a data-driven method. To solve the above problems, this paper proposes a health status prediction method based on the belief rule base (BRB) for the running gear system. First, a failure mechanism is analyzed to confirm the fault characteristics, which can represent the health status of the running gear system. Second, in order to avoid the limitations of a single sensor acquisition, such as a lack of comprehensiveness and robustness, singular value decomposition is used to achieve multisensory information fusion. The fused features are used as the input to the health status prediction model. Data fusion is a way to improve the precision of the health status prediction in the model input. Then, this model based on the BRB is established using the fault data and expert knowledge. During the process of prediction, the subjectivity of experts makes the initial BRB imprecise, so a projection constrained covariance matrix adaptive evolution strategy algorithm is needed to optimize the initial parameters and improve the accuracy of the proposed model. Finally, a case study for the running gear system is carried out to verify the effectiveness and accuracy of the proposed model. The results show that the proposed model can help to accurately predict the health status of the running gear system.

INDEX TERMS Belief rule base, projection constrained covariance matrix adaptive evolution strategy, fatal degree, singular value decomposition, health status prediction.

I. INTRODUCTION

As the key equipment of a high-speed train, the failure of the traveling section will affect the safety and comfort of the high-speed train, and even make it possible to run off the track [1], [2]. A reasonable prediction of the health status of a running gear can effectively improve the safety and reliability of the system. Additionally, it can prevent casualties and economic losses due to failures [3], [4]. Therefore, this paper studies the health status prediction of a high-speed train's running gear system to improve the reliability of the running gear and guarantee the safe operation of the high-speed train.

A high-speed train's traveling section is typically a complex electromechanical system with many units and complex structures. Currently, the common health status prediction methods for complex electromechanical systems are divided into three categories: analytical model-based methods, data-driven approach and qualitative knowledge-based approach [5]–[7]. Methods based on analytical models include such as Kalman filtering [8], [9]. By analyzing the mechanism of the system, a nonlinear analytical model is established to make a reasonable prediction of the next step of the system. However, this kind of method relies too

heavily on the mechanism analysis of the research object, and it is very difficult to directly establish an analytical model for a complex electromechanical system. Recently, the data-driven intelligent learning model has been developed rapidly and is widely used. This kind of method can solve the prediction problem of complex nonlinear systems [10], [11] based on a large amount of monitoring data, such as the support vector machine (SVM) [12], [13] and the hidden Markov model (HMM) [14]. These are typical methods based on multivariable statistics, which use monitoring data to establish nonlinear prediction models of complex systems and judge system faults by failure thresholds [15], [16], thus predicting the future status of the system. The models of the BP neural network and artificial neural network (ANN) [17]–[19] are based on non-statistical quantitative analysis methods and do not require knowing the corresponding knowledge in advance, thus simplifying the complexity of the problem. The above mentioned data-driven methods have a simple modeling mechanism and high prediction accuracy for some problems when predicting the health status of complex systems. However, such methods lack an explanation for the mechanism of system changes when they have a large amount of monitoring data, making it difficult to identify small patterns from large-scale data and resulting in a poor generalization ability of the system. There are some methods based on qualitative analysis. For example, the document in [20] and [21] proposes a prediction model based on a fault tree analysis and establishes several fault trees according to different fault categories in order to predict the failure mode of the system. However, when this type of method is used to deal with complex systems, the branch calculation is complex, which makes qualitative analysis difficult. The expert system method is the most commonly used qualitative knowledge model. Due to an insufficient analysis of quantitative knowledge containing a qualitative analysis, the prediction results are not very accurate. Although the above method can solve the problem of the health status prediction of a high-speed train traveling section through the data-driven method, in the traveling section system, there are only small-scale failure data in a large number of monitoring data, and the effective modal data are insufficient, resulting in inaccurate prediction results. It is difficult to construct a health prediction model to reflect the dynamic changes of future behavior by means of a mechanism analysis because of the close coupling between components and the complex structure in the traveling department system. Therefore, to solve the problem where the existing methods only consider the limitation of a single knowledge, fuzzy, uncertain information, etc., Yang *et al.* described the belief rule base modeling concept [22] based on the evidence reasoning method [23] on the basis of the D-S theory [24], fuzzy theory [25] and the traditional IF-THEN rule base, where the confidence level is introduced and combined with expert knowledge to reflect the behavior of the complex system. A rule base [26], [27] containing all the confidence levels of the results can well deal with the problem of the health status prediction of the complex system [28]. To this end, this paper proposes a BRB-prediction model based on the health status for a high-speed train running gear system, which uses semiquantitative information to establish a health status prediction model for the system. A singular value decomposition is used to fuse multisensory information. The singular value after the decomposition cannot correctly correspond to the information of the sensor, and the singular value is updated by the QR decomposition, so that the information corresponding to each sensor is accurately obtained, and the accuracy of the fusion result is improved, the fused features are used as inputs of the prediction model. The parameters of the models are optimized using the P-CMA-ES algorithm [29]. This method constructs a new prediction model containing semiquantitative information, which not only objectively describes the system but also accurately predicts the health status.

This article is arranged as follows: in the second part, the failure mode of the traveling section system and the fatal degree of the monitorable components are analyzed and then are reasonably selected as the key characteristic quantity of the high-speed train's health status. In the third part, a health prediction model for the high-speed train running gear is proposed. The fourth section gives the actual verification of predicting the health status of the high-speed train traveling section and illustrates the effectiveness of the proposed algorithm, followed by concluding remarks in the last section

II. MECHANISM ANALYSIS OF HIGH-SPEED TRAIN RUNNING GEAR

The main task of the high-speed train running gear system is to maintain the high-speed stability of the train operation and reduce the wheel-rail interaction force. Its structure diagram is shown in Fig. 1 below.

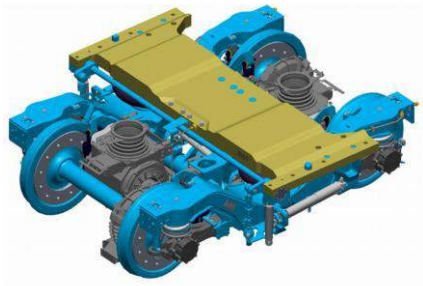

FIGURE 1. Diagram of the high-speed train running gear system.

In the running gear system. the frame carries the installation of various parts of the running gear and also bears various forces during the running. Including the wheelset in direct contact with the rail, the gravity of the carriage and the adhesion traction force and braking force between the rail and the frame is the frame of the running gear, and the wheelset makes the high-speed train run normally on the rail through rotation, which makes the axle box device connecting the frame and the wheelset components especially important. The axle box is the key equipment for ensuring the free rotation of the wheelset and the normal running of the high-speed train,

which is also the key equipment for ensuring operational safety.

For the sake of restoring the real running status of various parts of the train running gear, according to a large amount of maintenance data collected by the General Administration of Railways in a certain year, classification processing was performed to obtain the fault location and fault type table of the high-speed train running gear, as shown in Table 1.

It is obvious from Table 1 that there are a total of 40 failure modes and 98 specific failures in the running gear system, among which the wheel-to-axle box positioning device includes 33 shafts and axle boxes, which account for 33.6% of faults. It can be seen from Table 1 that the axle box device has a high failure rate in several running components, but the true situation in the failure mode cannot be obtained. Although, according to Table 1, we understand the failure mode and the cause of the train running gear, it is still unclear how fatal the failure mode is for each running function. Therefore, the analysis can monitor the lethality of the components to grasp the real operation of the key components, and intuitively reflect the health of the high-speed train.

When component i fails in failure mode j, the fatal degree of the component is:

$$\mathrm{CR}_{ij} = \alpha_{ij}\beta_{ij}\lambda_i \tag{1}$$

The component i in failure mode j; β_{ij} is the probability of a loss in the function condition that component i will cause component damage in failure mode j. If its value is 1, it means that damage must occur. Possible damage is indicated by 0.5; 0.1 indicates that damage will rarely occur; and 0 means no effect. λ_i is the average failure rate used for the component i to become a basic failure component. Its calculation formula is:

$$\lambda_i = \frac{n_i}{\sum_{j=1}^{m} T_j} \tag{2}$$

where n_i is the total number of failures of component i within the specified time, T_j is the j_{th} fault interval in the fault interval time series of component i within the specified time, and m is the number of fault intervals.

After processing and calculation, the fatal degree analysis results of monitorable components in a high-speed train operation are shown in Table 2.

The other components in Table 2, including those with lower dead lies such as couplings and brake calipers, have a lower risk of failure. Among the detectable components in operation, the axle box is the most lethal mainly because it bears the connection between the frame and the wheelset, and the vibration triggered by the indirect contact between the components during the running of the train easily damages the axle box device. In addition, the vibration of the bearings during operation, poor lubrication, and other factors will cause the shaft temperature to exceed its limit, changing the internal structure of the component material. The bearing is connected to the wheelset group in the running gear system, so the key components such as the axle box and other components will be slightly rubbed. This causes an additional vibration of the bearing. Therefore, the shaft temperature and bearing vibration are selected as two important features of the system. Due to the lack of comprehensiveness and

TABLE 1. Statistics of failure modes of running gear system.

Failure mode	Frequency / time	Percentage %	Effective percentage %	Cumulative percentage %
Safety valve air leakage	1	1.02	1.02	1.02
Wheel tread damage	2	2.04	2.04	3.06
Abnormal wear of shaft grounding device	6	6.12	6.12	9.18
There are oil marks on the shaft end	2	2.04	2.04	11.22
Oil level observation window leaks oil	1	1.02	1.02	12.24
Gearbox damage	2	2.04	2.04	14.28
The waterproof retainer ring of the gearbox comes out	1	1.02	1.02	15.3
Oil leakage from gearbox	2	2.04	2.04	17.34
Auxiliary air compressor connector failure	1	1.02	1.02	18.36
The height control valve leaks oil	1	1.02	1.02	19.38
Frame crack	1	1.02	1.02	20.4
The baffle is damaged	1	1.02	1.02	21.42
Lateral shock absorber leaks oil	3	3.06	3.06	24.48
The ventilator vibrates greatly	1	1.02	1.02	25.5
Anti - snake connecting rod damage	1	1.02	1.02	26.52
Anti - hunting shock absorber oil leakage	8	8.16	8.16	34.68
Anti - hunting shock absorber failure	1	1.02	1.02	35.7
Air spring failure	1	1.02	1.02	36.72
Air spring air leakage	3	3.06	3.06	39.78
Wheel set tread defect	1	1.02	1.02	40.8
Wheel set abrasion	9	9.18	9.18	49.98
Oil leakage from wheel disc	3	3.06	3.06	53.04
Disc damage	1	1.02	1.02	54.06
Speed sensor failure	3	3.06	3.06	57.12
Failure of tread cleaning device	1	1.02	1.02	58.14
Compression device failure	1	1.02	1.02	59.16
The brake caliper leaks oil	1	1.02	1.02	60.18
Brake duct support weld break	1	1.02	1.02	61.2
Brake clamp clearance is too small	1	1.02	1.02	62.22
Shaft brake shoe temperature is too high	1	1.02	1.02	63.24
Defect detection of hollow shaft	4	4.08	4.08	67.32
Shaft disc damage	4	4.08	4.08	71.4
Shaft box anti-vibration rubber deformation	1	1.02	1.02	72.42
Shaft box front cover failure	3	3.06	3.06	75.48
The shaft box body is provided with grease	4	4.08	4.08	79.56
Shaft box bearing temperature overrun	14	14.32	14.32	93.88
Cracks in the bearings of the primary suspension shaft box	2	2.04	2.04	95.92
Axle box bolt missing	1	1.02	1.02	96.94
Main transformer fault	1	1.02	1.02	97.96
Main transformer oil leakage	2	2.04	2.04	100
Total	98	100	100	

TABLE 2. Analysis fatal degree of monitorable components (part).

Parts	Failure mode	Cause of failure	Fault effect	α_{ij}	β_{ij}	Model lethality $/10^{-4}\cdot h$	$\lambda_i/10^{-4}$	Component lethality $/10^{-4}\cdot h$
axle box body	Cassette injury	Operating environment	Axle box damage	0.038	0.1	0.069	6.512	2.57224
	Axle box front cover cracked	Operating environment	Axle box damage	0.114	0.1	0.069	——	——
	Axle box anti-vibration rubber deformation	Operating environment	Anti - vibration effect becomes worse	0.038	0.5	0.344	——	——
	Shaft abrasion	Operating environment	Shaft damage	0.076	0.1	0.069	——	——
	Outer windshield rubber hole tear	Operating environment	Outer windshield effect is worse	0.038	0.1	0.344	——	——
	Axle box end cover deformation	Operating environment	Lubrication effect is affected	0.038	0.5	0.344	——	——
	Axle box bearing temperature overrun	Poor lubrication of shaft box bearings	Lubrication effect is affected	0.5	0.5	3.14	——	——
	debris in the hollow axle	Operating environment	easy to cause shaft injury	0.12	0.1	0.069	——	——
	Slight scratch on the bearing surface	Supplier manufacturing quality problems	Poor lubrication of shaft box bearings	0.038	0.1	0.069	——	——
Gearbox composition	Pinion outer cylinder offset with clearance	To be analyzed	Pro	0.14	0.5	0.321	4.356	1.934
	Oil leakage from gearbox	Operating environment	Lubrication effect is affected	0.3	0.5	0.642	——	——
	Oil level observation window leaks oil	Operating environment	Lubrication is worse	0.14	0.5	0.321	——	——
	Gearbox damage	Operating environment	Gearbox damage	0.28	0.5	0.642	——	——
	Gearbox grease expired	Improper use and maintenance	Lubrication is worse	0.14	0.1	0.0642	——	——
Lateral shock absorber	Lateral shock absorber leaks oil	Supplier manufacturing quality problem	Poor damping effect	1	0.5	1.586	4.125	2.0625
Traction rod composition	Rubber joint cracking	Operating environment	Affect the performance of the traction rod	0.5	1	1.14	2.69	1.4795
	Side rubber node breakage	Side rubber node breakage	Deteriorating rubber node performance	0.5	0.1	0.856	——	——

robustness of single sensor acquisition, multisensory information fusion will be used to reflect the train health status. In the health prediction BRB model, the initial parameters need to be set through expert knowledge and historical data. However, as the result of a limitation in expert knowledge, the initial parameters are indefinite. Therefore, the

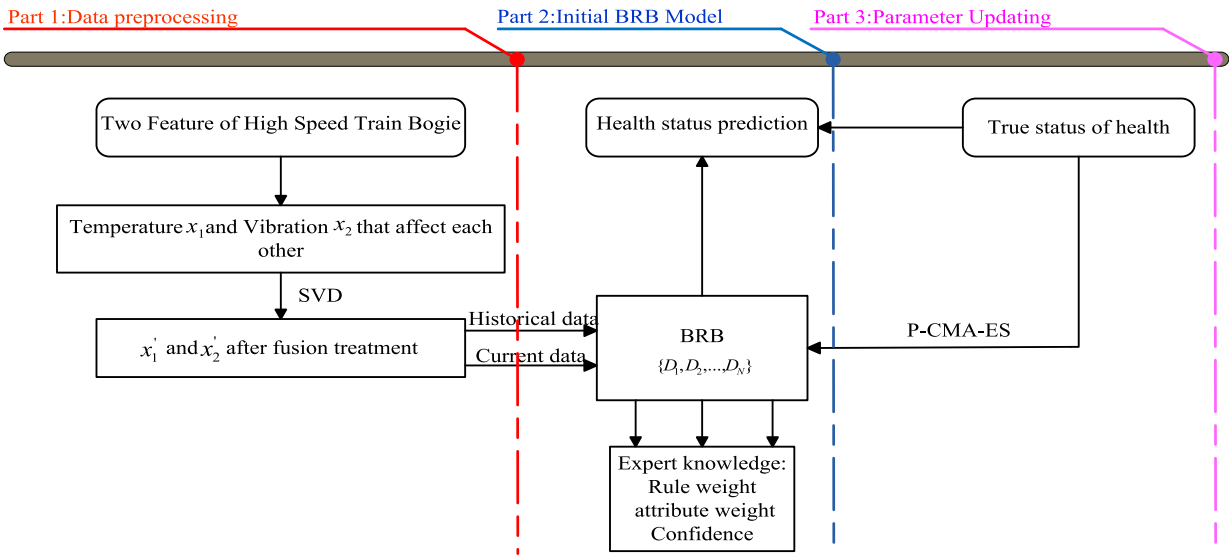

FIGURE 2. Flow chart of health prediction modeling for high-speed train running gear system.

optimization of initial parameters can update the prediction model more accurately, reflecting the running gear, i.e., the actual operating status of the system.

III. HIGH-SPEED TRAIN RUNNING GEAR HEALTH PREDICTION MODEL

For the sake of predicting the true health of a high-speed train at runtime, a model with semiquantitative information is proposed to process the prediction problem. As shown in Fig. 2, the structure of the model is mainly divided into three parts. In the first part, after the data collected by different measuring points are merged, a health status prediction model is established as a key feature input model. In the second part, based on faulty data and expert knowledge, a BRB health prediction model is constructed. The initial parameters in the model are updated using P-CMA-ES.

A. DATA FUSION

For the sake of reducing the errors caused by environmental factors, such as sensor quality, and restore the real health status of trains, multisource sensor data are fused. A more effective method of data fusion is a singular value decomposition, which can preserve the original trend while ensuring that the abnormal point is eliminated. It has six steps, as follows:

Step 1: Build an input matrix $\mathbf{M}$ of multisensory measurement results.

$$\mathbf{M} = [\mathbf{M}_1, \mathbf{M}_2, \cdots, \mathbf{M}_N] = \begin{bmatrix} \mathbf{M}_1(1) & \mathbf{M}_2(1) & \cdots & \mathbf{M}_N(1) \\ \mathbf{M}_1(2) & \mathbf{M}_2(2) & \cdots & \mathbf{M}_N(2) \\ \vdots & \vdots & \ddots & \vdots \\ \mathbf{M}_1(l) & \mathbf{M}_2(l) & \ldots & \mathbf{M}_N(l) \end{bmatrix} \tag{3}$$

where $\mathbf{M}_i$ represents the observation result of the i_{th} sensor, The data acquisition value of the traveling section. $i = 1, 2, \cdots, N$.

Step 2: Denoise with the LOF (local outlier factor) [30] to obtain the input matrix.

$$\text{reach-dist}_k(p, o) = \max\{k - \text{dist}(o), d(p, o)\} \tag{4}$$

$$\text{lrd}_k(p) = 1/\left(\frac{\sum_{o \in N_k(p)} \text{reach-dist}_k(p, o)}{|N_k(p)|}\right) \tag{5}$$

$$\begin{aligned} \text{LOF}_k(p) &= \frac{\sum_{0 \in N_k(p)} \frac{\text{lrd}_k(o)}{\text{lrd}_k(p)}}{|N_k(p)|} \\ &= \frac{\sum_{0 \in N_k(p)} \text{lrd}_k(o)}{|N_k(p)|} / \text{lrd}_k(p) \end{aligned} \tag{6}$$

$$\begin{aligned} \tilde{\mathbf{M}} &= [\tilde{\mathbf{M}}_1, \tilde{\mathbf{M}}_2, \cdots, \tilde{\mathbf{M}}_N] \\ &= \begin{bmatrix} \tilde{\mathbf{M}}_1(1) & \tilde{\mathbf{M}}_2(1) & \cdots & \tilde{\mathbf{M}}_N(1) \\ \tilde{\mathbf{M}}_1(2) & \tilde{\mathbf{M}}_2(2) & \cdots & \tilde{\mathbf{M}}_N(2) \\ \vdots & \vdots & \ddots & \vdots \\ \tilde{\mathbf{M}}_1(l) & \tilde{\mathbf{M}}_2(l) & \ldots & \tilde{\mathbf{M}}_N(l) \end{bmatrix} \end{aligned} \tag{7}$$

where $d(p, o)$ represents the Euclidean distance between o and p, $d_k(p)$ represents the kth distance of the point of p, $N_k(p)$ represents the kth distance neighborhood of the point of p, reach-dist$_k(p, o)$ represents the kth reachable distance from point o to point p, lrd$_k(p)$ represents the local reachable density of point p, and LOF$_k(p)$ represents the local outlier of the point of p. If LOF$_k(p) \gg 1$, the point p is determined to be an abnormal point or an invalid point, Then all the abnormal points in the data set $\mathbf{M}$ that meet the p point requirement are eliminated, and $n < l$, the input matrix $\tilde{\mathbf{M}}$ is updated after LOF processing.

Step 3: Calculate the singular value of the sensor observation matrix $\widetilde{\mathbf{M}}$.

$$\begin{aligned}\mathbf{U}\widetilde{\mathbf{M}}\mathbf{V} &= \mathrm{diag}(\sigma_1, \cdots, \sigma_p) \in R^{n\times N}, \quad p = \min\{n, N\},\\ \widetilde{\mathbf{M}} &= \mathbf{V}\mathbf{J}\mathbf{U}^{\mathrm{T}}, \quad \mathbf{J} = \mathrm{diag}(\sigma_1, \cdots, \sigma_p) \in R^{n\times N},\\ \mathbf{P} &= \mathrm{rank}(\widetilde{\mathbf{M}})\end{aligned} \tag{8}$$

where the orthogonal arrays $\mathbf{U} = [u_1, \cdots, u_N] \in R^{n\times n}$ and $\mathbf{V} = [v_1, \cdots, v_N] \in R^{N\times N}$ are singular vectors of $\widetilde{\mathbf{M}}$, the diagonal matrix $\mathbf{J}$ is the singular value matrix of $\widetilde{\mathbf{M}}$, the diagonal element $\boldsymbol{\sigma}_p$ corresponds to the column vector of each input matrix $\widetilde{\mathbf{M}}$.

Step 4: Determine the singular value σ_p and the position in the input matrix $\widetilde{\mathbf{M}}$ by QR decomposition [27].

$$\begin{aligned}\mathbf{B} &= \mathbf{U}^{\mathrm{T}}\widetilde{\mathbf{M}}, \widetilde{\mathbf{M}} \in R^{n\times N}, n > N\\ \mathbf{B} &= (\mathbf{B}^{\mathrm{T}})^{\mathrm{T}} = (\mathbf{Q}_B\mathbf{R}_B)^{\mathrm{T}} = \mathbf{R}_B^{\mathrm{T}}\mathbf{Q}_B^{\mathrm{T}}\\ \widetilde{\mathbf{M}} &= \mathbf{U}\mathbf{J}_1\mathbf{V}^{\mathrm{T}}\\ \mathbf{J}_1 &= \mathrm{diag}(\sigma_1', \sigma_2', \cdots, \sigma_p') \in R^{n\times N}\end{aligned} \tag{9}$$

where $\mathbf{B}$ is a row vector orthogonal matrix, updating $\mathbf{J}_1 = \mathbf{R}_B^{\mathrm{T}}$, $\mathbf{V}^T = \mathbf{Q}_B^T$ and a singular value σ_p'.

Step 5: Calculate the influence weight W_p of each sensor

If $n < N$, then $p = 1, 2, \cdots, N$.

$$W_p = \frac{\sigma_p'}{\sum_{p=1}^{N}\sigma_p'}$$

$$\sum_{p=1}^{N} W_p = 1 \tag{10}$$

where σ_p' is the singular value of N sensors.

Step 6: Calculate the estimated quantity $\mathbf{M}$ after data fusion of N sensors

$$\hat{\mathbf{M}} = \sum_{p=1}^{N} W_p \cdot \underset{p}{\widetilde{\mathbf{M}}} \tag{11}$$

B. INITIAL BRB MODEL FOR HEALTH STATUS PREDICTION OF RUNNING GEAR SYSTEM

By combining the known detection data with the base rules, the process provides more information than the IF-THEN rule operation by introducing parameters such as premise attribute weights, rule weights, and confidence, which is the calculation method of the actual situation.

The model k rule is expressed as

If $x_1(t+\tau)$ is $R_1^k \wedge x_2(t+\tau)$ is $R_2^k \wedge \cdots \wedge x_M(t+\tau)$ is R_M^k

Then $\{(D_1, \psi_{1,k}), \cdots, (D_N, \psi_{N,k})\}$

With a rule weight θ_k and attribute weight

$$\delta_1, \cdots, \delta_M \tag{12}$$

where x_i denotes the i_{th} bogie fault characteristic vector. τ is the delay step. Based on expert prior knowledge and historical data. R^k denotes a set of reference values entered by k_{th} rule $R^k = \{R_1^k, \cdots, R_M^k\}$, $(k = 1, \cdots, L)$. Where L denotes the total number of rules. $\psi_{n,k}(n = 1, \cdots, N)$ denotes belief degree by which D_i is considered as the result whether $(x_1(t+\tau), \cdots, x_M(t+\tau)) = (R_1^k, \cdots, R_M^k)$, M is the number of estimation results. D denotes a status vector for health prediction. And $D = [D_1, \cdots, D_N]$, where N denotes the amount of status s including the normal status of the system.

In the process of BRB reasoning, an evidence Reasoning analysis [28] method is used. In an ER analysis algorithm, confidence can be obtained directly.

Step 1: Calculate the confidence of the premise attribute $\chi_{i,j}^k$ relative to the reference value.

$$\chi_{i,j}^k(x_i^*) = \begin{cases} \dfrac{x_{i(k+1)} - x_i^*}{x_{i(k+1)} - x_{ik}}, & j = k(x_{ik} \le x_i \le x_{i(k+1)})\\ \dfrac{x_i^* - x_{ik}}{x_{i(k+1)} - x_{ik}}, & j = k+1\\ 0, & j = 1, 2, \cdots, |x_i|,\ j \ne k, k+1 \end{cases} \tag{13}$$

where $w_k \in [0, 1], k = 1, 2, \cdots, L$, $\chi_{i,j}^k$ is the matching degree of the rule-based or utility-based input information with respect to the i_{th} premise attribute of the j_{th} rule.

Step 2: Calculation method of activation weight w_k in the k_{th} rule.

$$w_k = \frac{\theta_k \prod_{i=1}^{M} (\chi_i^k)^{\bar{\delta}_i}}{\sum_{l=1}^{L} \theta_l \prod_{i=1}^{M} (\chi_i^l)^{\bar{\delta}_i}} \tag{14}$$

where $w_k \in [0, 1], k = 1, 2, \cdots, L$, $\bar{\delta}_i$ is attribute weight.

Step 3: Using ER algorithm for reasoning, we can get the output of BRB.

$$S(x) = \{(D_N, \hat{\psi}_j), j = 1, 2, \cdots, N\} \tag{15}$$

$$\hat{\psi}_j = \frac{\mu \cdot [\prod_{k=1}^{L}(w_k\psi_{j,k} + 1 - w_k\sum_{i=1}^{M}\psi_{i,k}) - \prod_{k=1}^{L}(1 - w_k\sum_{i=1}^{M}\psi_{i,k})]}{1 - \mu \cdot [\prod_{k=1}^{L}(1 - w_k)]} \tag{16}$$

$$\mu = [\sum_{j=1}^{N}\prod_{k=1}^{L}(w_k\psi_{j,k} + 1 - w_k\sum_{i=1}^{M}\psi_{i,k}) - (N-1) \times \prod_{k=1}^{L}(1 - w_k\sum_{k=1}^{N}\psi_{i,k})]^{-1} \tag{17}$$

$$y = \mu(S(x)) = \sum_{j=1}^{N}\mu(D_N)\psi_j \tag{18}$$

where $S(x)$ is the final output of the BRB model, $\hat{\psi}_j$ represents the confidence level relative to the evaluation result D_N,

y is the expected utility of the $S(x)$ of the high-speed train running gear.

C. PARAMETER UPDATE ALGORITHM BASED ON P-CMA-ES

The health status y is solved and the MSE objective function in (19).

$$\vartheta(J) = \frac{1}{T-\tau}\sum_{t=\tau+1}^{T}\left(y(t) - \hat{y}(t)\right)^2 \tag{19}$$

where $\mathbf{J} = [\theta_k, \delta_i, \psi_{n.k}, \mu(D_n)]^{\mathrm{T}}$ denotes a column vector composed of the parameters in BRB, T is the amount of data, and $\theta_k, \delta_i, \psi_{n,k}, D_n$ are set up.

For the sake of making $\hat{y}$ fit y_n as much as possible, obtain the following objective function.

$$\min \vartheta(\mathbf{J}) \tag{20}$$

The constraints are as follows:

$$\begin{aligned}
&\min \vartheta(\mathbf{J})\\
&s.t.\ \sum_{n=1}^{N}\psi_{n,k} = 1\\
&\quad 0 \le \psi_{n,k} \le 1, \quad n = 1, 2, \cdots, N;\ k = 1, 2, \cdots, L\\
&\quad 0 \le \delta_i \le 1, \quad i = 1, 2, \cdots, M_k\\
&\quad 0 \le \theta_k \le 1, \quad k = 1, 2, \cdots, L
\end{aligned} \tag{21}$$

where $\theta_k, \psi_{n,k}$ are gave in (19), min() denotes the minimum value of $\vartheta(\mathbf{J})$, and δ_i is the estimated reference value of attribute weights.

Use the P-CMA-ES algorithm to constrain the optimization objective function, and then optimize the proposed model. The combination of CMA-ES and the projection matrix can deal with the constraint problem, reduce the complexity of the model and optimize the population convergence rate.

The specific optimization steps are as follows:

Step 1: Sampling produces new solutions. Set the sampled population to the expected value, and the population conforms to the normal distribution where the initial expectation is the parameter vector $\mathbf{J}$ of the initial BRB model.

$$J_q^{g+1} \sim mean^g + \upsilon^g N(0, \mathbf{C}^g)(q = 1, \cdots, \rho) \tag{22}$$

where g is the updated g_{th} expectation mean, υ is the updated step size, and $\mathbf{C}$ is the covariance matrix to be updated.

Step 2: Projection operation.

$$\begin{aligned}
&\Omega_i^{g+1}(1 + z_e \times (u-1) : z_e \times u)\\
&\quad = \Omega_i^{g+1}(1 + z_e \times (u-1) : z_e \times u)\\
&\qquad - B_i^T \times (B_e \times B_e^T)^{-1} - B_e^T \times (B_e \times B_e^T)^{-1}\\
&\qquad \times \Omega_i^{g+1}(1 + z_e \times (u-1) : z_e \times u) \times B_e
\end{aligned} \tag{23}$$

where $\mathbf{B}_e = [1 \cdots 1]_{1\times 2^N}$ is the parameter vector, $z_e = (1, \cdots, 2^Z)$ is the number of constraint variables, and $u = (1, \cdots, 2^Z + 1)$ is the number of constraint.

Step 3: Multi-objective constraints. Update the objective function to be optimized according to the constraint. That is, the confidence level of the k_{th} rule in the constraint parameter vector J_q, where $\psi_{n,k} \in J_q$, $\sum_{n=1}^{N}\psi_{n,k} = 1$.

The constraint objective function is

$$S_k(\psi_{n,k}) = \left|\sum_{n=1}^{N}\psi_{n,k} - 1\right| \tag{24}$$

where $S_k(\psi_{n,k})$ is the constraint function to be optimized for the k_{th} rule in the initial BRB.

Step 4: Exchange information and reorganize between different solutions. Combine the selected partial solutions to obtain the next-generation mean, and then update the target mean and select φ as the updated mean value of the optimal solution.

$$mean^{g+1} = \sum_{i=1}^{\phi}\tau_i J_{i:\lambda}^{g+1} \tag{25}$$

where τ is the individual weight, and the sum of all weights is 1; λ is the individual number, and $J_{i:\lambda}^{g+1}$ is the i_{th} solution chosen from λ individuals in $g+1$ generation.

Step 5: Adjust the covariance matrix.

$$\begin{aligned}
\mathbf{C}^{g+1} &= (1 - a_1 - a_\phi)\mathbf{C}^g + a_1 f^{g+1}(f^{g+1})^{\mathrm{T}}\\
&\quad + a_\phi \sum_{i=1}^{\phi}\tau_i\left(\frac{(J_{i:\lambda}^{g+1} - mean^g)}{\upsilon^g}\right)\left(\frac{(J_{i:\lambda}^{g+1} - mean^g)}{\upsilon^g}\right)^{\mathrm{T}}
\end{aligned} \tag{26}$$

where a_1 and $a_\phi$are learning factors, and f is the evolutionary path.

Set the initial parameters of the evolutionary path to 0 according to (26) and then update parameter f.

$$\begin{aligned}
f^{g+1} &= (1 - a_p)f^g + \sqrt{a_p\left(2 - a_p\right)\left(\sum_{i=1}^{\phi}\tau_i^2\right)^{-1}}\\
&\quad \times \frac{mean^{g+1} - mean^g}{\upsilon^g}
\end{aligned} \tag{27}$$

where $a_p \le 1$ is the updated parameter of the evolutionary path and υ is the evolutionary step size.

$$\upsilon^{g+1} = \upsilon^g \exp\left(\frac{a^\upsilon}{d_\upsilon}\left(\frac{\left\|f_\upsilon^{g+1}\right\|}{E\left\|N(0, \mathbf{I})\right\|}\right)\right) \tag{28}$$

where d_υ is the damping coefficient, $E\left\|N(0, \mathbf{I})\right\|$ is the expectation of $\|N(0, \mathbf{I})\|$, and I is the identity matrix.

$$\begin{aligned}
f_\upsilon^{g+1} &= (1 - a_\upsilon)f_\upsilon^g + \sqrt{a_\upsilon(2 - a_\upsilon)(\sum_{i=1}^{\tau}\tau_i^2)^{-1}\mathbf{C}^{(g)-\frac{1}{2}}}\\
&\quad \times \frac{mean^{g+1} - mean^g}{\upsilon^g}
\end{aligned} \tag{29}$$

where a_υ is the parameters of evolutionary path f_υ.

Step 6: Iteration.

Through steps 1-5, the most suitable parameter set is determined. If the condition of the optimal solution is not met, the

process returns to step 1 and the update is performed until the condition is met. Then, finish updating parameter set **J**.

D. CONSTRUCTION STEPS OF THE HEALTH PREDICTION MODEL FOR HIGH-SPEED TRAIN RUNNING GEAR SYSTEM

According to the above analysis, four steps of the health prediction model of the high-speed train running gear are as follows:

Step 1: Multisensory Data Information Fusion

Step 1-1: Establish an input matrix **M** of multi-sensor measurement results (3).

Step 1-2: Use LOF to denoise and get the input matrix $\tilde{\mathbf{M}}$ (4-7).

Step 1-3: Calculate the singular value of sensor observation matrix $\tilde{\mathbf{M}}$ (8).

Step 1-4: Use QR decomposition to determine the position of singular value σ_p and input matrix $\tilde{\mathbf{M}}$ (9).

Step 1-5: Calculate the influence weight W_p of each sensor (10).

Step 1-6: Calculate the estimated quantity $\hat{\mathbf{M}}$ after data fusion of N sensors (11).

Step 2: Establish a BRB health model with initial parameters.

Step 2-1: Experts give attribute weights, reference values and initial confidence levels according to expert knowledge.

Step 2-2: Establish a BRB-based health prediction model.

Step 3: The parameters are updated using the P-CMA-ES algorithm.

Step 3-1: Sampling produces new solutions (22).

Step 3-2: Projection operation (23).

Step 3-3: Multi-objective constraints (24).

Step 3-4: Exchange information and reorganize between different solutions (25).

Step 3-5: Adjusting the covariance matrix (26-29).

Step 3-6: Iteration. Finish updating parameter set **J**.

Step 4: The ER analysis algorithm is used for health prediction to obtain a status of health including confidence.

The high-speed train travel system was set up, and the axle box temperature rise and vibration were finally selected to characterize the health status of the high-speed train travel section. Since the attribute weight measures the importance of the health status, if the health status of the high-speed train is estimated, the vibration of the axle box is as important as the temperature rise. the attribute weight can be determined to be 1. Assume that the reference value is set to five levels to measure the change in the predictive input and to predict the health of the system. As a complex electromechanical system, the health department is subdivided into five types. The more reference values, the more detailed the process of describing the status of health changes. The fourth section describes the expert knowledge setting process through cases.

IV. ACTUAL VERIFICATION

For the sake of verifying the validity and reliability of the semiquantitative information model proposed in this paper, the high-speed train running system is taken as an example for practical verification. When the data acquisition of the running gear is selected, the side of the power running gear of train No. 2 is selected for sampling. Fig. 3 shows the position distribution of the sensor points and the sampling point position. A and B are the two measuring points of the running gear. They are divided into left (L) and right (R), and the composite sensor is installed on both sides. For the sake of ensuring the train is in operation, the monitoring data with a rotational speed of 1000 r/min or above is verified as a model. As the high-speed train running system is affected by the operating environment during real operation, the health status of the high-speed train running gear will be measured, which is defined as "Health," "Wheel Repair," "Temporary Repair," "Garage Repair," "Stop to Repair."

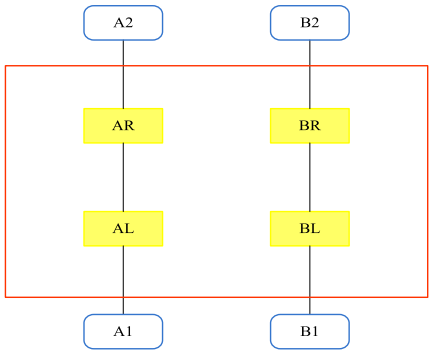

FIGURE 3. Distribution of axle box measuring points on bogies.

A. DATA FUSION

In the actual monitoring data, there are singular points in different measuring points due to factors such as sensor quality problems and the location of points, as shown in Fig. 4 with (a), (b). For the sake of making the monitoring data better reflect the health status of the system, (3-11) is now used to fuse multisensory features, filter out relevant singular points without destroying the original features of the data, reduce errors caused by external factors, and finally compress 1000 data volumes, as shown in Fig. 5 with (a), (b).

B. BRB TRAINING MODEL

The five health statuses of a high-speed train running system are defined as follows:

Health: All parts of the high-speed train work well and fasteners do not loosen that all indicators meet the factory requirements. When the train is in this status, the temperature and vibration are normal, and the amplitude is low, so the high-speed train can ensure safe running.

Wheel Repair: The parts slightly wear and shaped during operation. When the train is in this status, the average vibrational peak is between 10-13 Hz and the temperature

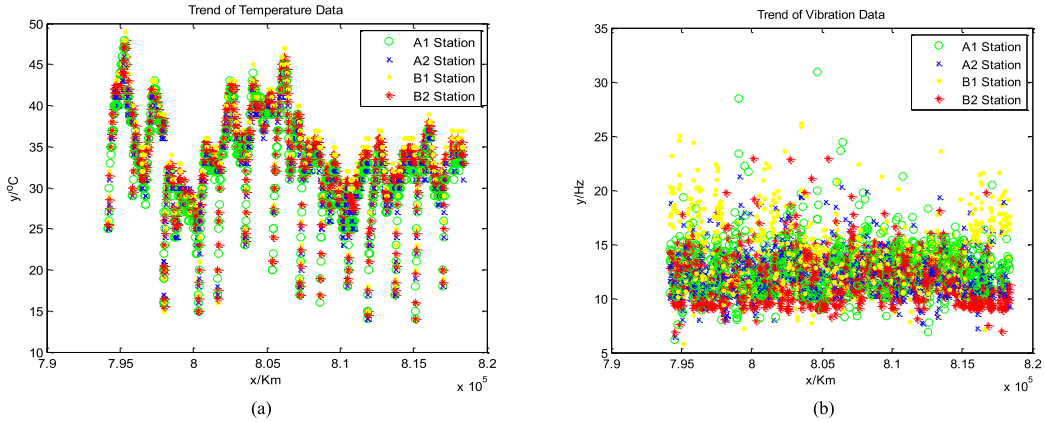

FIGURE 4. Trend diagram of four measuring points. (a) Temperature (b) Vibration.

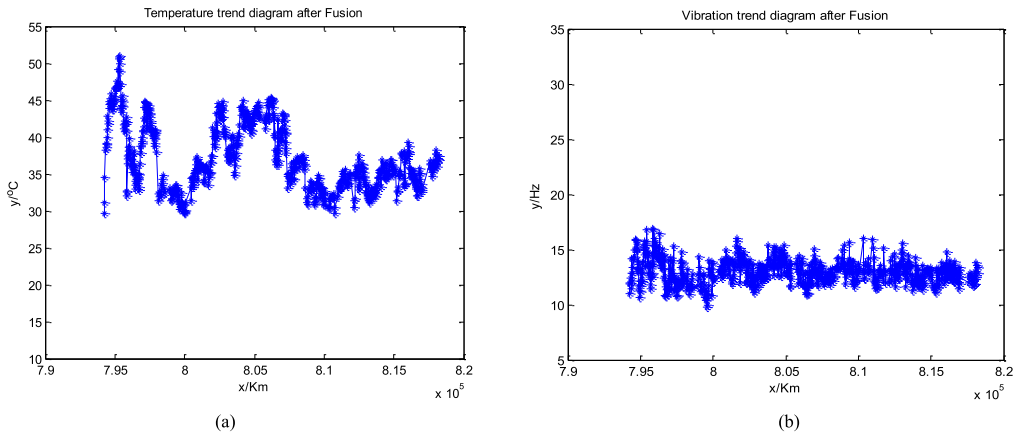

FIGURE 5. Trend diagram after fusion. (a) Temperature (b) Vibration.

TABLE 3. The referential points.

Temperature		Vibration		Health status	
Referential points	Referential values	Referential points	Referential values	Referential points	Referential values
VL	13	VL	7	H	1
L	21	L	11	WR	2
M	30	M	15	TR	3
H	39	H	19	GR	4
VH	48	VH	23	STR	5

is between 20 $°C$-27 $°C$. Checking of appearance, working condition and general performance of every part work for preventive and corrective maintenance. Under this status, the normal running will not effect.

Temporary Repair: High-speed train reaches a tipping point of health and malfunction. When the train is in this status, the average vibration peak value is between 13 and 16 Hz and the temperature is between 27 $°C$-34 $°C$. In accordance with the relevant regulations of the Train repair and repair system, the train needs periodically repair and adjust the systems and components without disassembling the wheels in the next maintenance to ensure the normal running of the train.

Garage Repair: The running function of high-speed train decreases and some parts are in a bad status, which may lead to failure. When the train is in this status, the average peak value of vibration is between 16-19 Hz, and the temperature is between 34 $°C$-41$°C$. As the check seek to improve the safety of the train. It is necessary to replace or repair the parts of the train that are monitored.

Stop to Repair: The components of the train are seriously damaged, and the operation will stop at any time. When the

TABLE 4. Initial BRB parameter setting.

Rule Number	Rule weights	R_1 and R_2	Health Status Distribution $\{D_1, D_2, D_3, D_4, D_5\} = \{1, 2, 3, 4, 5\}$
1	1	VL AND VL	$\{(D_1,1),(D_2,0),(D_3,0),(D_4,0),(D_5,0)\}$
2	1	VL AND L	$\{(D_1,0.9),(D_2,0.1),(D_3,0),(D_4,0),(D_5,0)\}$
3	1	VL AND M	$\{(D_1,0.7),(D_2,0.3),(D_3,0),(D_4,0),(D_5,0)\}$
4	1	VL AND H	$\{(D_1,0.5),(D_2,0.5),(D_3,0),(D_4,0),(D_5,0)\}$
5	1	VL AND VH	$\{(D_1,0.3),(D_2,0.7),(D_3,0),(D_4,0),(D_5,0)\}$
6	1	L AND VL	$\{(D_1,0.1),(D_2,0.9),(D_3,0),(D_4,0),(D_5,0)\}$
7	1	L AND L	$\{(D_1,0),(D_2,1),(D_3,0),(D_4,0),(D_5,0)\}$
8	1	L AND M	$\{(D_1,0),(D_2,0.9),(D_3,0.1),(D_4,0),(D_5,0)\}$
9	1	L AND H	$\{(D_1,0),(D_2,0.7),(D_3,0.3),(D_4,0),(D_5,0)\}$
10	1	L AND VH	$\{(D_1,0),(D_2,0.5),(D_3,0.5),(D_4,0),(D_5,0)\}$
11	1	M AND VL	$\{(D_1,0),(D_2,0.3),(D_3,0.7),(D_4,0),(D_5,0)\}$
12	1	M AND L	$\{(D_1,0),(D_2,0.1),(D_3,0.9),(D_4,0),(D_5,0)\}$
13	1	M AND M	$\{(D_1,0),(D_2,0),(D_3,1),(D_4,0),(D_5,0)\}$
14	1	M AND H	$\{(D_1,0),(D_2,0),(D_3,0.9),(D_4,0.1),(D_5,0)\}$
15	1	M AND VH	$\{(D_1,0),(D_2,0),(D_3,0.7),(D_4,0.3),(D_5,0)\}$
16	1	H AND VL	$\{(D_1,0),(D_2,0),(D_3,0.5),(D_4,0.5),(D_5,0)\}$
17	1	H AND L	$\{(D_1,0),(D_2,0),(D_3,0.3),(D_4,0.7),(D_5,0)\}$
18	1	H AND M	$\{(D_1,0),(D_2,0),(D_3,0.1),(D_4,0.9),(D_5,0)\}$
19	1	H AND H	$\{(D_1,0),(D_2,0),(D_3,0),(D_4,1),(D_5,0)\}$
20	1	H AND VH	$\{(D_1,0),(D_2,0),(D_3,0),(D_4,0.9),(D_5,0.1)\}$
21	1	VH AND VL	$\{(D_1,0),(D_2,0),(D_3,0),(D_4,0.7),(D_5,0.3)\}$
22	1	VH AND L	$\{(D_1,0),(D_2,0),(D_3,0),(D_4,0.5),(D_5,0.5)\}$
23	1	VH AND M	$\{(D_1,0),(D_2,0),(D_3,0),(D_4,0.3),(D_5,0.7)\}$
24	1	VH AND H	$\{(D_1,0),(D_2,0),(D_3,0),(D_4,0.1),(D_5,0.9)\}$
25	1	VH AND VH	$\{(D_1,0),(D_2,0),(D_3,0),(D_4,0),(D_5,1)\}$

train is in this status, the average peak value exceeds 19 Hz, and the temperature exceeds 41 $°C$. At this status, emergency braking is needed, and the parts of the train monitored should be repaired immediately to prevent dangerous situations.

In the BRB model, not only are the vibration and temperature indexes important to the health prediction of the high-speed train running system but also the rule set is equally important, so α_k, R_2 can be assigned to 1. When setting the reference values for vibration and temperature, the number of reference values determines the number of rules, and an increase in the number of rules will lead to the complexity of model calculation. According to expert knowledge, the set temperature has five reference levels, including VL (Very Low), L (Low), M (Medium), H (High), and VH (Very High), expressed as VL, L, M, H and VH, with the attribute values listed in Table 3. The set vibration is also expressed as five reference levels VL, L, M, H and VH, and the attribute values are listed in Table 3. The health status reference levels

TABLE 5. BRB parameters optimized by P-CMS-EA.

Rule Number	Rule weights	R_1 and R_2	Health Status Distribution $\{D_1, D_2, D_3, D_4, D_5\} = \{1, 2, 3, 4, 5\}$
1	0.9872	VL AND VL	$\{(D_1,0.8853),(D_2,0.0984),(D_3,0.0102),(D_4,0.0037),(D_5,0.0025)\}$
2	0.0105	VL AND L	$\{(D_1,0.1204),(D_2,0.2692),(D_3,0.0865),(D_4,0.4707),(D_5,0.0532)\}$
3	0.0835	VL AND M	$\{(D_1,0.2845),(D_2,0.0713),(D_3,0.3961),(D_4,0.0045),(D_5,0.2436)\}$
4	0.6629	VL AND H	$\{(D_1,0.5547),(D_2,0.0337),(D_3,0.1419),(D_4,0.1960),(D_5,0.0737)\}$
5	0.4518	VL AND VH	$\{(D_1,0.4522),(D_2,0.1163),(D_3,0.0420),(D_4,0.3797),(D_5,0.0099)\}$
6	0.5415	L AND VL	$\{(D_1,0.5387),(D_2,0.1572),(D_3,0.2930),(D_4,0.0023),(D_5,0.0089)\}$
7	0.0260	L AND L	$\{(D_1,0.0705),(D_2,0.0122),(D_3,0.5571),(D_4,0.1293),(D_5,0.2309)\}$
8	0.8960	L AND M	$\{(D_1,0.8338),(D_2,0.0699),(D_3,0.0364),(D_4,0.0475),(D_5,0.0124)\}$
9	0.5869	L AND H	$\{(D_1,0.3444),(D_2,0.3591),(D_3,0.0479),(D_4,0.0956),(D_5,0.1529)\}$
10	0.3776	L AND VH	$\{(D_1,0.1110),(D_2,0.1087),(D_3,0.2796),(D_4,0.0687),(D_5,0.4319)\}$
11	0.5231	M AND VL	$\{(D_1,2573),(D_2,0.1450),(D_3,0.0789),(D_4,0.3338),(D_5,0.1850)\}$
12	0.1624	M AND L	$\{(D_1,0.2032),(D_2,0.2308),(D_3,0.5074),(D_4,0.0566),(D_5,0.0021)\}$
13	0.8266	M AND M	$\{(D_1,0),(D_2,0.2591),(D_3,0.5407),(D_4,0.1660),(D_5,0.0345)\}$
14	0.3228	M AND H	$\{(D_1,0.1897),(D_2,0.2321),(D_3,0.0103),(D_4,0.2724),(D_5,0.2955)\}$
15	0.0831	M AND VH	$\{(D_1,0.3319),(D_2,0.1725),(D_3,0.0652),(D_4,0.1178),(D_5,0.3126)\}$
16	0.0484	H AND VL	$\{(D_1,0.0603),(D_2,0.2003),(D_3,0.1876),(D_4,0.3854),(D_5,0.1664)\}$
17	0.2672	H AND L	$\{(D_1,0.0687),(D_2,0.0881),(D_3,0.0036),(D_4,0.2999),(D_5,0.5397)\}$
18	0.6719	H AND M	$\{(D_1,0.5049),(D_2,0.2352),(D_3,0.1657),(D_4,0.0413),(D_5,0.0529)\}$
19	0.0022	H AND H	$\{(D_1,0.0602),(D_2,0.0732),(D_3,0.0046),(D_4,0.5036),(D_5,0.3583)\}$
20	0.6204	H AND VH	$\{(D_1,0.0125),(D_2,0.1656),(D_3,0.1605),(D_4,0.0632),(D_5,0.5983)\}$
21	0.4646	VH AND VL	$\{(D_1,0.0001),(D_2,0.0071),(D_3,0.0750),(D_4,0.6116),(D_5,0.3062)\}$
22	0.1023	VH AND L	$\{(D_1,0.2427),(D_2,0.0061),(D_3,0.2228),(D_4,0.1028),(D_5,0.4257)\}$
23	1	VH AND M	$\{(D_1,0),(D_2,0),(D_3,0.0021),(D_4,0.0107),(D_5,0.9923)\}$
24	0.2052	VH AND H	$\{(D_1,0.2074),(D_2,0.0724),(D_3,0.1633),(D_4,0.1439),(D_5,0.4131)\}$
25	0.4876	VH AND VH	$\{(D_1,0.1384),(D_2,0.2927),(D_3,0.2225),(D_4,0.1165),(D_5,2298)\}$

output for the BRB model include H (Health), WR (Wheel repair), TR (Temporary repair), GR (Garage repair), and STR (Stop to repair), expressed as H, WR, TR, GR, and STR, with the attribute values listed in Table 3.

The temperature and vibration reference values are divided into five levels, with a total of 25 confidence rules. According to expert knowledge, the health prediction the BRB model of a high-speed train running gear is established.

The K_{th} rule can be described as:

$$R_k: \ \textit{If Temperature is } R_1^k \ \wedge \ \textit{Vibration is } R_2^k$$
$$\textit{Then health status is } \{(1, \psi_{1,k}), (2, \psi_{2,k}), (3, \psi_{3,k}), (4, \psi_{4,k}), (5, \psi_{5,k})\}$$
$$\left(\sum_{n=1}^{N} \psi_{n,k} \leq 1\right) \quad k \in \{1, \cdots, 25\}$$

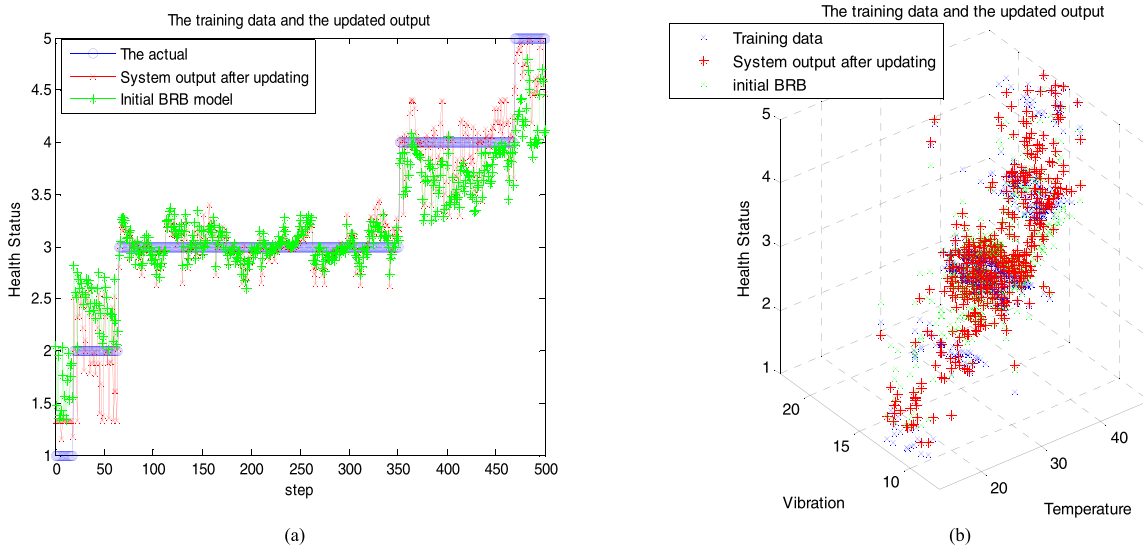

FIGURE 6. Two results of the initial BRB model (a) result 1 (b) result 2.

According to expert knowledge, Table 4 sets the initial parameters of the BRB model. For example, when the vibration amplitude is large and the temperature is high, the health of the high-speed train running gear is poor. The first rule, VL AND VL, means that the temperature and vibration are in a very low status and remain normal. The health status of the high-speed train running gear system should remain healthy. Thus, the health status of the high-speed train running gear is assigned to $\{(D_1, 1), (D_2, 0), (D_3, 0), (D_4, 0), (D_5, 0)\}$. The seventh rule, explains the gradual change from health to the "Wheel repair" of the running gear system of the high-speed train running gear. L AND L indicate that both the temperature and vibration are decreased to a low level, and the health status of the high-speed train running gear system is in "Wheel repair." Therefore, the health status of the high-speed train running gear is given $\{(D_1, 0), (D_2, 1), (D_3, 0), (D_4, 0), (D_5, 0)\}$.

In the parameter training of BRB, 500 data were selected from the data set, and the model parameters were updated using the P-CMA-ES algorithm; with the population size set to 90 and the number of iteration set to 500. The parameters in the BRB model were updated as shown in Table 5 after training. The presumed attribute weights for $\mathbf{x}_1$ and $\mathbf{x}_2$ are updated to 1 and 0.6155, respectively. The red line from Fig. 6 (a) represents the optimized BRB model output, the blue line represents the true status of the system, the green line represents the output of the initial BRB model, it can be seen from the resulting graph that the red line is more effective than the green line, and the blue line is well fitted, thus verifying the effectiveness of the optimized BRB model. As shown in Fig. 6 (b), the red dot is more suitable than the green dot to fit the real situation represented by the blue dot. Therefore, the trained model can better predict the health of the system.

C. BRB TEST MODEL

The test data includes 500 data points. From Fig. 7 (a) and (b), the red line can track the trend of the blue line more than the green line. According to the result, it can be change of the test data, and the optimized BRB prediction determined that the prediction result can well follow the result has more than the initial BRB. A good fit confirms the effectiveness of optimizing the BRB model. The mean squared error (MSE) of the optimized BRB model is set to 0.1045. Therefore, it is obvious that the optimized BRB model can more reasonably predict the health of the system.

D. COMPARATIVE SIMULATION

For the sake of further testifying to the validity of the model, a classical data-driven method was used to compare and analyze the proposed method. The BP neural network and particle filtering model are used to predict the health status of the high-speed train running components, and the feasibility of the proposed model to solve the practical industrial problems is verified. The initial value of the parameters' BP neural network is set as follows: net. Train Param. epochs=500, net. Train Param. goal=0.01 and net. Train Param. lr=0.15. The health status levels are also defined as 1, 2, 3, 4, and 5, denoted as Health, Wheel repair, Temporary repair, Garage repair, and Stop to repair, respectively.

Fig. 8 (a) is a comparison of the dynamic change prediction of the BP neural network compared to the optimized BRB model. According to the dynamic change prediction results of the BP neural network, it can be concluded that BP neural network can initially follow the blue line to predict fit is better, but the fluctuations are large in the "Garage repair" and "Stop to Repair," and it is impossible to accurately track changes and predict the health status. Compared with the

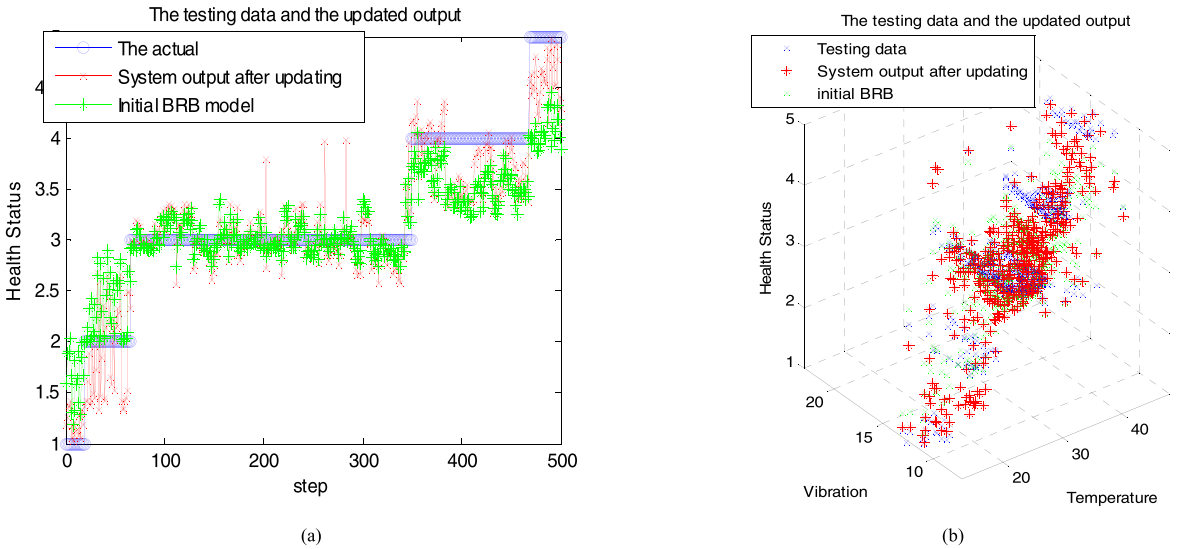

FIGURE 7. Two results of the trained BRB model (a) result 1 (b) result 2.

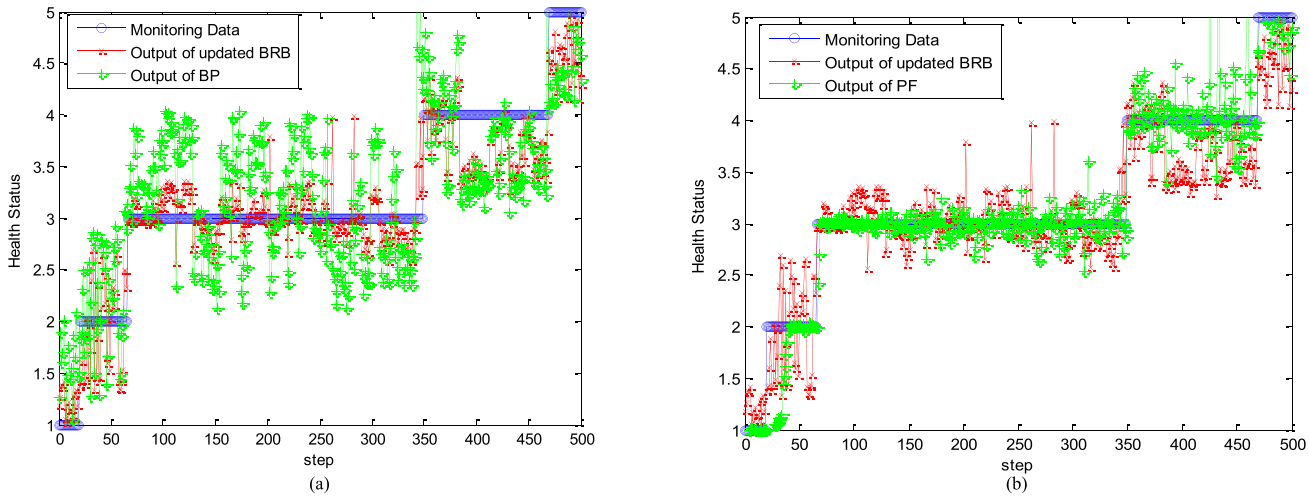

FIGURE 8. Comparison with other models (a) with BP (b) with PF.

TABLE 6. The MSE of models.

Models	MSE
Initial BRB	0.1645
The updated BRB	0.1045
BP	0.5925
Particle Filtering	0.3249

green line, the red line can accurately track the blue line and predict its health status.

V. CONCLUSION

This paper proposes a predictive model based on semiquantitative information, which is used to predict the its change, but it fluctuates greatly in the "Temporary Repair" status and cannot be accurate. The track changes and predicts the health status. Compared to the green line, the red line can accurately track the blue line and predict its health.

The particle filter model for predictive analysis and the initial particle number M=10 can be seen in Fig. 8 (b). In the "Temporary Repair" status of the Train Param. lr=0.15. The health status levels are also defined as 1, 2, 3, 4, and 5, denoted as Health, Wheel repair, Temporary repair, Garage repair, and Stop to repair, respectively.

Fig. 8 (a) is a comparison of the dynamic change prediction of the BP neural network compared to the optimized BRB model. According to the dynamic change prediction results of the BP neural network, it can be concluded that BP neural network can initially follow the blue line to predict its change, but it fluctuates greatly in the ''Temporary Repair'' status and cannot be accurate. The track changes and predicts the health status. Compared to the green line, the red line can accurately track the blue line and predict its health.

The particle filter model for predictive analysis and the initial particle number M=10 can be seen in Fig. 8 (b). In the ''Temporary Repair'' status of the system, the degree of health status of the high-speed train running gear during actual operation. By analyzing the fault mode and fatality of the train running system, the real-time key features are obtained. Due to the quality of the sensor and the location of the distribution point, the data of the existing measurement points are fused, and the relevant singular points are filtered out without reducing the original features of the data, thereby reducing the error caused by external factors. By using the BRB model to establish the contact between the health status and quantitative fault data and expert knowledge, the P-CMA-ES algorithm is introduced to solve the problem of parameter inaccuracy in the BRB model given by experts, optimize the structure of the model, and improve the prediction accuracy.

An example analysis based on the health status prediction of the traveling section of high-speed trains shows that the BRB system trained with the optimization model proposed in this paper can predict the health status of the traveling section system well, and the model has a high applicability to practical engineering problems. It provides a new solution for practical engineering that cannot obtain a large number of effective monitoring data through expert knowledge to predict the health status of complex systems.

For the sake of verifying the feasibility of the model, two common data-driven methods, the BP neural network and particle filtering model, are compared with the proposed model. The results show that the model proposed in this paper has a high accuracy in the health prediction of a high-speed train running gear. The model combines the corresponding expert knowledge in front of a large amount of historical data and current data to effectively predict the health status of the high-speed train running gear in actual industrial processes.

When using the BRB model, it is necessary to ensure that the model inputs are independent of one another, which is conducive to the establishment of a complete rule base. However, in the actual industrial process, the input features of the model may not be completely independent of one another. When predicting the health status of high-speed trains, the prediction accuracy is better than the traditional method. However, when the actual situation is considered, further research should be conducted so as to account for the potential correlation between feature quantities.

REFERENCES

[1] M. Torabi, S. G. M. Mousavi, and D. Younesian, ''A high accuracy imaging and measurement system for wheel diameter inspection of railroad vehicles,'' *IEEE Trans. Ind. Electron.*, vol. 65, no. 10, pp. 8239–8249, Oct. 2018, doi: 10.1109/TIE.2018.2803780.

[2] Z. Chen, S. X. Ding, T. Peng, C. Yang, and W. Gui, ''Fault detection for non-Gaussian processes using generalized canonical correlation analysis and randomized algorithms,'' *IEEE Trans. Ind. Electron.*, vol. 65, no. 2, pp. 1559–1567, Feb. 2018.

[3] C. D. Dao and M. J. Zuo, ''Optimal selective maintenance for multi-state systems in variable loading conditions,'' *Rel. Eng. Syst. Saf.*, vol. 166, pp. 171–180, Oct. 2017.

[4] J. Xi, C. Wang, H. Liu, and Z, Wang, ''Dynamic output feedback guaranteed-cost synchronization for multiagent networks with given cost budgets,'' *IEEE Access*, vol. 6, pp. 28923–28935, Apr. 2018.

[5] C. Lu, L. Tao, and H. Fan, ''An intelligent approach to machine component health prognostics by utilizing only truncated histories,'' *Mech. Syst. Signal Process.*, vol. 42, nos. 1–2, pp. 300–313, 2014, doi: 10.1016/j.ymssp.2013.08.025.

[6] L. Lu, J. Yan, and Y. Meng, ''Dynamic genetic algorithm-based feature selection scheme for machine health prognostics,'' *Procedia CIRP*, vol. 56, pp. 316–320, Jan. 2016.

[7] J. B. Yu, ''Machine health prognostics using the Bayesian-inference-based probabilistic indication and high-order particle filtering framework,'' *J. Sound Vib.*, vol. 358, pp. 97–110, Sep. 2015.

[8] X. He, Z. Wang, X. Wang, and D. H. Zhou, ''Networked strong tracking filtering with multiple packet dropouts: Algorithms and applications,'' *IEEE Trans. Ind. Electron.*, vol. 61, no. 3, pp. 1454–1463, May 2014.

[9] T. Soubdhan, J. Ndong, H. Ould-Baba, and M.-T. Do, ''A robust forecasting framework based on the Kalman filtering approach with a twofold parameter tuning procedure: Application to solar and photovoltaic prediction,'' *Sol. Energy*, vol. 131, pp. 246–259, Jun. 2016.

[10] D. Zhou, H. Ji, X. He, and H. Shang, ''Fault detection and isolation of the brake cylinder system for electric multiple units,'' *IEEE Trans. Control Syst. Technol.*, vol. 26, no. 5, pp. 1744–1757, Sep. 2018.

[11] H. Q. Ji, X. He, J. Shang, and D. H. Zhou, ''Incipient sensor fault diagnosis using moving window reconstruction-based contribution,'' *Ind. Eng. Chem. Res.*, vol. 55, no. 10, pp. 2746–2759, Feb. 2016.

[12] A. Shebani and S. Iwnicki, ''Prediction of wheel and rail wear under different contact conditions using artificial neural networks,'' *Wear*, vols. 406–407, pp. 173–184, Jan. 2018.

[13] K. Sun, G. Li, H. Chen, J. Liu, J. Li, and W. Hu, ''A novel efficient SVM-based fault diagnosis method for multi-split air conditioning system's refrigerant charge fault amount,'' *Appl. Therm. Eng.*, vol. 108, pp. 989–998, Sep. 2016.

[14] F. Wang, S. Tan, Y. Yang, and H. Shi, ''Hidden Markov model-based fault detection approach for a multimode process,'' *Ind. Eng. Chem. Res.*, vol. 55, no. 16, pp. 4613–4621, Mar. 2016.

[15] Q. Jiang, X. Yan, and B. Huang, ''Performance-driven distributed PCA process monitoring based on fault-relevant variable selection and Bayesian inference,'' *IEEE Trans. Ind. Electron.*, vol. 63, no. 1, pp. 377–386, Jan. 2016.

[16] Q. Jiang and X. Yan, ''Parallel PCA–KPCA for nonlinear process monitoring,'' *Control Eng. Pract.*, vol. 80, pp. 17–25, Nov. 2018.

[17] N. Daroogheh, A. Baniamerian, N. Meskin, and K. Khorasani, ''Prognosis and health monitoring of nonlinear systems using a hybrid scheme through integration of PFs and neural networks,'' *IEEE Trans. Syst., Man, Cybern. A, Syst. Humans*, vol. 47, no. 8, pp. 1990–2004, Aug. 2017.

[18] Y. Aslan and Y. E. Yağan, ''Artificial neural-network-based fault location for power distribution lines using the frequency spectra of fault data,'' *Elect. Eng.*, vol. 99, no. 1, pp. 301–311, Sep. 2016.

[19] L. Jin, C. Peng, and T. Jiang, ''System-level electric field exposure assessment by the fault tree analysis,'' *IEEE Trans. Electromagn. Compat.*, vol. 59, no. 4, pp. 1095–1102, Aug. 2017.

[20] C. Mao, F. G. Canavero, Z. Cui, and D. Sun, ''System-level vulnerability assessment for EME: From fault tree analysis to Bayesian networks—Part II: Illustration to microcontroller system,'' *IEEE Trans. Electron. Compat.*, vol. 58, no. 1, pp. 188–196, Feb. 2016.

[21] R. Landau, ''Intelligent fault diagnosis at the Australia telescope,'' *Publications Astron. Soc. Aust.*, vol. 11, no. 2, pp. 180–187, Jul. 2016.

[22] J. B. Yang, J. Liu, J. Wang, H. S. Sii, and H. W. Wang, ''Belief rule-base inference methodology using the evidential reasoning approach-RIMER,'' *IEEE Trans. Syst., Man, Cybern. A, Syst., Humans*, vol. 36, no. 2, pp. 266–285, Feb. 2006.

[23] Z.-G. Liu, Q. Pan, J. Dezert, and A. Martin, "Combination of classifiers with optimal weight based on evidential reasoning," *IEEE Trans. Fuzzy Syst.*, vol. 26, no. 3, pp. 1217–1230, Jun. 2018.
[24] L. Oukhellou, A. Debiolles, T. Denœux, and P. Aknin, "Fault diagnosis in railway track circuits using Dempster–Shafer classifier fusion," *Eng. Appl. Artif. Intel.*, vol. 23, no. 1, pp. 117–128, Feb. 2010.
[25] L. Sun, Z. Ma, Y. Shang, Y. Liu, H. Yuan, and G. Wu, "Research on multi-attribute decision-making in condition evaluation for power transformer using fuzzy AHP and modified weighted averaging combination," *IET Gener., Transmiss. Distrib.*, vol. 10, no. 15, pp. 3855–3864, 2016.
[26] Z.-J. Zhou, C.-H. Hu, G.-Y. Hu, X.-X. Han, B.-C. Zhang, and Y.-W. Chen, "Hidden behavior prediction of complex systems under testing influence based on semiquantitative information and belief rule base," *IEEE Trans. Fuzzy Syst.*, vol. 23, no. 6, pp. 2371–2386, Dec. 2015.
[27] Z.-J. Zhou, G.-Y. Hu, B.-C. Zhang, C.-H. Hu, Z.-G. Zhou, and P.-L. Qiao, "A model for hidden behavior prediction of complex systems based on belief rule base and power set," *IEEE Trans. Syst., Man, Cybern. A, Syst. Humans*, vol. 48, no. 9, pp. 1649–1655, Sep. 2018.
[28] X. Yin *et al.*, "A double layer BRB model for health prognostics in complex electromechanical system," *IEEE Access*, vol. 5, pp. 23833–23847, 2017.
[29] G. Y. Hu, "Study on network security situation awareness based on belief rule base," Ph.D. dissertation, Dept. CST, Harbin Univ. Sci. Technol., Harbin, China, 2016.
[30] M. M. Breunig, H.-P. Kriegel, R. T. Ng, and J. Sander, "LOF: Identifying density-based local outliers," in *Proc. ACM SIGMOD Int. Conf. Manage. Data*, vol. 29, no. 2, 2000, pp. 93–104, doi: 10.1145/335191.335388.
[31] J. Yen and L. Wang, "An SVD-based fuzzy model reduction strategy," in *Proc. IEEE 5th Int. Fuzzy Syst.*, New Orleans, LA, USA, vol. 2, Sep. 1996, pp. 835–841, doi: 10.1109/FUZZY.1996.552288.
[32] Y.-M. Wang, J.-B. Yang, and D.-L. Xu, "Environmental impact assessment using the evidential reasoning approach," *Eur. J. Oper. Res.*, vol. 174, no. 3, pp. 1885–1913, 2006.

CHAO CHENG received the B.Eng. degree from Dalian Minzu University, Dalian, China, in 2007, and the M.Eng. and Ph.D. degrees from Jilin University, Changchun, China, in 2011 and 2014, respectively.

He is currently a Teacher with the Changchun University of Technology, Changchun. He has been a Post-Doctoral Fellow in process control engineering with the Department of Automation, Tsinghua University, Beijing, China, since 2018. He has also been a Post-Doctoral Fellow with the National Engineering Laboratory, CRRC Changchun Railway Vehicles Co., Ltd., China, since 2018.

His research interest includes dynamic system fault diagnosis and predictive maintenance, wireless sensor network, artificial intelligence, and data-driven method.

JIUHE WANG received the B.Eng. degree from the Changchun University of Technology, Changchun, China, in 2014, where he is currently pursuing the M.Eng. degree in computer science and engineering.

His research interests include complex system fault prediction, health status prediction, and belief rule base.

WANXIU TENG received the B.Eng. and M.Eng. degrees from Southwest Jiaotong University, Chengdu, China, in 2002 and 2010, respectively, where he is currently pursuing the Ph.D. degree in mechanical engineering. He has been a Party Branch Secretary and the Deputy Director of the National Engineering Laboratory, CRRC Changchun Railway Vehicles Co., Ltd., China, since 2015. His research interests include mechatronics measurement technique and fault diagnosis.

MINGLIANG GAO received the B.Eng. degree from Jilin University, Changchun, China, in 2011, and the M.Eng. and Ph.D. degrees from Jilin University, in 2015.

He has been a Data Supervisor with the National Engineering Laboratory, CRRC Changchun Railway Vehicles Co., Ltd., China, since 2015. He has been a Post-Doctoral Fellow in process control engineering with the Department of Automation, Tsinghua University, since 2018. His research interests include vehicle track big data analysis.

BANGCHENG ZHANG received the B.Eng. and M.Eng. degrees from the Changchun University of Technology, Changchun, China, in 1995 and 2004, respectively, and the Ph.D. degree from Jilin University, Changchun, in 2011.

He is currently a Professor with the Changchun University of Technology. He has been an Academic Visitor with Tsinghua University, Beijing, China, since 2007. He has published over 20 articles.

His research interests include mechatronics measurement technique and fault diagnosis.

XIAOJING YIN received the B.Eng. degree from the Liren College, Yanshan University, Qinhuangdao, China, in 2011, and the M.Eng. degree from the School of Mechatronic Engineering, Changchun University of Technology, Changchun, China, in 2014, where she is currently pursuing the Ph.D. degree in mechanical engineering. Her research interests include complex system fault diagnosis and prediction, health estimation, and prognostics.

HAO LUO received the B.E. degree in electrical engineering from Xi'an Jiaotong University, China, in 2007, the M.Sc. degree in electrical engineering and information technology from the University of Duisburg-Essen, Germany, in 2012, and the Ph.D. degree from the Institute for Automatic Control and Complex Systems, University of Duisburg-Essen, in 2016.

He is currently an Associate Professor with the School of Astronautics, Harbin Institute of Technology. His research interests include model-based and data-driven fault diagnosis, fault-tolerant systems, and their plug-and-play application on industrial systems.